2018 International Conference on Unmanned Aircraft Systems (ICUAS)
Dallas, TX, USA, June 12-15, 2018

Toward Lab Automation Drones for Micro-plate Delivery in High Throughput Systems

Dongbin Kim[1] and Paul Y. Oh[2]

Fig. 1. High Throughput Screening Laboratoy (Platebutler-Lab Services)

Fig. 2. Lab Automation Drone concept design

***Abstract*— In this paper, the author presents a lab automation drone concept design for high throughput systems(HTS). A 6 degree-of-freedom (6-DOF) parallel manipulator and parallel sensorized gripper are affixed together to a rotorcraft. The manipulator-gripper allows dexterously delivery of micro-plates broadly used for sample-testing in high throughput systems. For testing and evaluation, the concept design is deployed in two pick-and-place experiments using micro-plates. First the manipulator-gripper system is attached to a gantry crane system, then it is tested on a quadcopter under manual flight within motion capture space. The results demonstrate the viability of the design and point towards future work on stability controls for autonomous flight.**

I. Introduction

In lab automation, there are many possibilities for including robots, especially with high throughput systems(HTS) as seen in Fig. 1. In such a system, robotic arms continuously and dexterously load micro-plates into sample testing stations. Over many years, the use of these robotic arms has enabled high throughput and more complex experiments to be run on lab automation systems.In the big data era, high throughput screening is very important for faster biochemistry and pharmaceutical development.

However, robotic arms are not without limitation, despite their tremendous benefit to a HTS environment. Once the HTS is configured with robotic arms, it is hard to change because it is usually customized for different HTS demands. This is important because older HTS can not easily perform new tests. The National Institutes of Health (NIH) in the United States is looking for the potential of lab automation drones to add flexibility to current HTS. The purpose is to create indoor autonomous drone capable of moving commonly used micro-plates from one location to another. The notion has merit because aerial manipulation and indoor navigation is an active area of robotics research, and issues such as ground effect, limited battery life, and obstacle avoidance are highly related to lab automation [1]-[3]. In previous work, the author focused on a manipulator-and-gripper concept design for lab automation drone [4]. The results show 95 percents precision at micro-plate pick-and-place. However, there is no test flight result with a lab automation drone concept. In this paper, the lab automation drone concept design from the previous work is deployed in two environments to pick-and-place micro-plates. One is affixed to a gantry crane system that emulates ideal autonomous flight path, another is deployed in manual flight with motion capture space. The results are compared. Section II describes related work; Section III describes hardware and software components; Section IV showcases testing and evaluation results; and Section V presents conclusion and discussion for future work.

II. Related Work

A typical HTS can handle over 500,000 samples a week, or more. Therefore, dexterous micro-plate delivery is significant for HTS. Today's state-of-the-art HTS employs high-precision robotic arms to manipulate micro-plates amongst numerous test-stations. The robotic arms are taught to move in pre-determined routes to deliver micro-plates. Fig. 3 shows the NIH Chemical Genomics Center (NCGC) robotic screening system. Three Staubli robotic arms are mounted to execute HTS protocols. The arm's parallel jaw gripper gently position and orient micro-plates [5], [6].

[1]Dongbin Kim is with Drones and Autonomous Systems Laboratory (DASL), University of Nevada Las Vegas, NV 89119, USA dongbin.kim@unlv.edu

[2]Paul Y. Oh is with Drones and Autonomous Systems Laboratoy (DASL), University of Nevada, Las Vegas, NV 89119, USA paul.oh@unlv.edu

978-1-5386-1353-5/18/$31.00 ©2018 IEEE

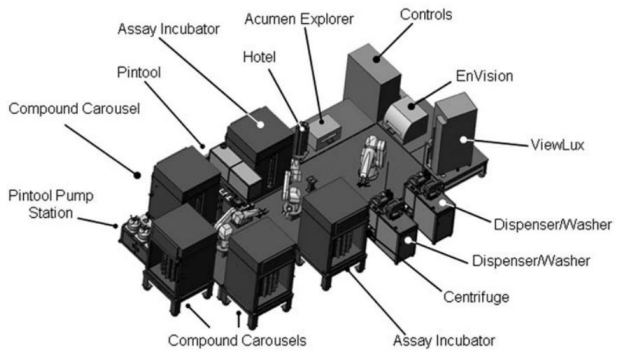

Fig. 3. NCGC robotic screening system

The ability of an unmanned aerial system (UAS) to interact physically with objects within its surroundings completely transforms the view of UAS applications in near-earth environments. This change in paradigm expands the types of mission achievable by UAS, such as aerial repair, construction, assembly, and disaster response. Several configuration systems have been explored to create aerial manipulation systems [7]-[9]. In [10],[11], autonomous indoor aerial manipulations are implemented using Simultaneous Localization And Mapping (SLAM), or state feedback from motion-capture system.

In previous work [4], the author presented parallel-mechanism robotic arm and parallel sensorized gripper for lab automation drones with precise micro-plate grasping. However, test flight results had yet to be reported. This paper begins reporting test flight results and discussing future testing and evaluation work.

III. Hardware and Software Design

A. Testing Lab Automation Drone Design Concept

The Q450 quadcopter frame is selected for the test flight. Four LD-Power 960kV motors with 24cm propellers are mounted on the frame. Additional landing gears are attached to create a 25cm square workspace under the quadcopter. 11.1kV, 2200mAh Li-Po battery is connected for power source. An open-source autopilot, *Pixhawk*, is mounted for flight control. The flight data is stored and downloaded on an open-source software, Mission Planner. The payload is estimated to be 3.0kg [12], so the author designed total weight of manipulator and gripper design less than 1kg because of .

The 6 degree-of-freedom(6-DOF) parallel manipulator is built with 8 servo motors. Table I shows the manipulator dimensions. The size is adjusted to quadcopter frame. All motors on the manipulator are controlled by the C++ open-source software, Pololu Mastro Servo Controller. In Fig. 4, the 8 legs attaching the base b to the moving platform p can be seen. All 8 motors work together to drive the mass of the legs and the moving platform. Each leg, i, is attached to a servo on the base by a revolute joint. The servo drives a fixed length link, D_1, to an angle θ_i from the plane of the base. The D_1 link is connected to a second fixed length link,

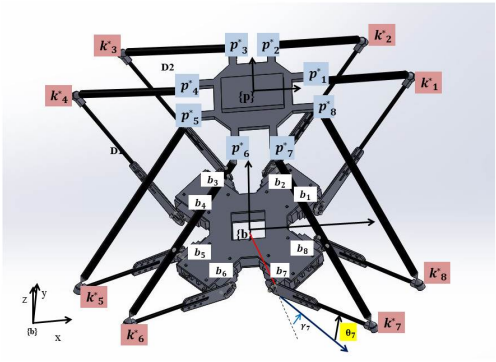

(a) CAD Design of the manipulator (inverted for clarity)

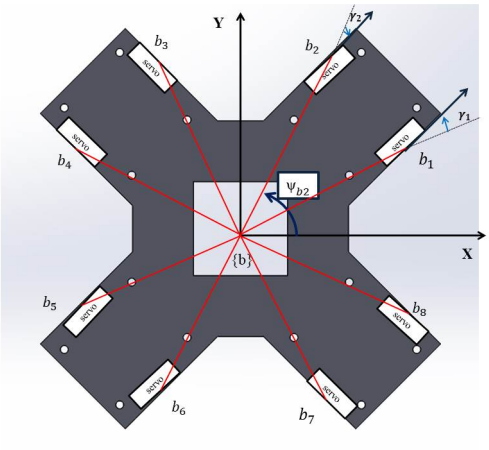

(b) Geometrical arrangement of leg attachment points

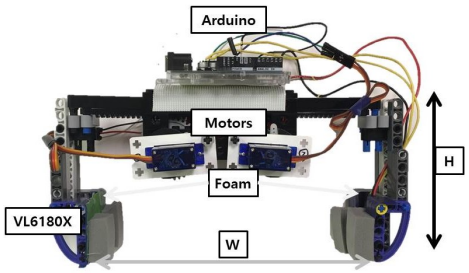

(c) Actual design of the manipulator

Fig. 4. Parallel manipulator and gripper concept design

D_2, via a spherical *knee* joint, and the other end of the D_2 link attaches to the platform via a second spherical joint. The relative mounting positions of each leg is described in terms of angles ψ_{bi} and ψ_{pi} in the xy plane. γ_i is an angle between ψ_{bi} and the position of the link on the xy base plane, D_1. Table II and III shows the coordinates of each leg attachment point. The manipulator is attached under the quadcopter.

The sensorized parallel jaw gripper is built for grasping work. Table IV shows the gripper dimension.The gripper

TABLE I

PHYSICAL PROPERTIES OF THE MANIPULATOR CONCEPT DESIGN

Symbol	Value	Description
D_1	0.110 m	Fixed length link (base joint and knee)
D_2	0.135 m	Fixed length link (knee and top platform joint)
L	0.773 m	Length (origin to the base attachment point)
M_{tm}	0.471 kg	Total mass of manipulator concept design
M_{mm}	0.093 kg	Total mass of moving components

TABLE II

ANGULAR COORDINATES OF LEG ATTACHMENT POINTS TO THE BASE AND MOVING PLATFORM

Leg(i)	$\psi_{bi}(radians)$	$\gamma_i(radians)$	$\psi_{pi}(radians)$
1	0.3658	0.4196	0.2782
2	1.2050	0.4196	1.2926
3	1.9336	0.4196	1.8490
4	2.7758	0.4196	2.8634
5	3.5074	0.4196	3.4198
6	4.3466	0.4196	4.4342
7	5.0781	0.4196	4.9906
8	5.9194	0.4196	6.0050

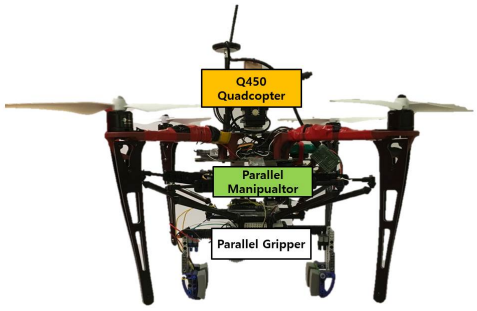

Fig. 5. Final Lab Automation Drone concept design

is operated by servo-motors that react to tactile feedback from an integrated-circuit(I^2C) compatible sensor, VL6180X (STMicroelectronics). The sensor is mounted left bottom side of the gripper in-hand. An I^2C compatible Arduino-Uno is connected to operate the gripper and receive proximity range data from the sensor. Two pieces of foams are attached on each side to enhance grasping characteristics. The grasping begins when the sensor receives proximity range data from the object. The gripper is mounted end-effector of the parallel manipulator.

The final concept design of lab automation drone is shown in Fig. 5.

TABLE III

LEG ATTACHMENT POSITIONS TO THE TOP AND BASE IN MANIPULATOR BASE COORDINATES

	Base Connections			Top Connections		
Leg(i)	$b_{xi}(m)$	$b_{yi}(m)$	$b_{zi}(m)$	$p_{xi}(m)$	$p_{yi}(m)$	$p_{zi}(m)$
1	0.0722	0.0277	0	0.0717	0.0205	0
2	0.0277	0.0722	0	0.0205	0.0717	0
3	-0.0277	0.0722	0	-0.0205	0.0717	0
4	-0.0722	0.0277	0	-0.0717	0.0205	0
5	-0.0722	-0.0277	0	-0.0717	-0.0205	0
6	-0.0277	-0.0722	0	-0.0205	-0.0717	0
7	0.0277	-0.0722	0	0.0205	-0.0717	0
8	0.0722	-0.0277	0	0.0717	-0.0205	0

TABLE IV

PHYSICAL PROPERTIES OF THE PARALLEL GRIPPER CONCEPT DESIGN

Symbol	Value	Description [m]
W	0.095-0.185m	Width between grip and non-grip
H	0.11 m	Height of the gripper
M_{tg}	0.234 kg	Total mass of the gripper concept design

B. Parallel Manipulator Kinematics

The parallel manipulator has 8-Revolute-Spherical-Spherical mechanisms (8-RSS). The inverse kinematics for this parallel manipulator is calculated to identify goal angles for each of the 8 driven revolute joints around the base platform that will drive the top platform to a desired pose in the manipulator's base coordinates. The work in [4], [14], and [15] describes kinematics of 8-RSS.

The homogeneous transform ${}^bT_p$ is used to take each leg's attachment point to the top platform, p_i, to its goal pose p_i^* in manipulator's base coordinates as shown in Eq. 1

$$p_i^* = p_i {}^bT_p \tag{1}$$

Next, the Euclidean distance L_i^* is calculated as the direct distance between b_i and p_i^* for each leg. L_i^* is a virtual leg, and it is the hypotenuse of the triangle formed by the points b_i, p_i^* and the knee, m_i^*.

$$L_i^* = ||p_i^* - b_i|| \tag{2}$$

Finally, the desired angle of servo rotation, θ_i, is calculated by Eq. 3

$$\theta_i = \arcsin\left(\frac{c}{\sqrt{a^2+b^2}}\right) - \arctan\left(\frac{b}{a}\right), \tag{3}$$

where:

$a = 2D_1(p_{zi}^* - b_{zi})$

$b = 2D_1[(p_{xi}^* - b_{xi})\cos(\psi_{bi} \pm \gamma_i) + (p_{yi}^* - b_{yi})\sin(\psi_{bi} \pm \gamma_i)]$

$c = L_i^{*2} - D_2^2 + D_1^2.$

In b, the sum of the angles is used in the sinusoids for legs L_1, L_3, L_5, and L_7, while the difference of the angles is used for legs L_2, L_4, L_6, and L_8.

Furthermore, it would be desirable to allow the manipulator lay against the base. This would facilitate grasping work

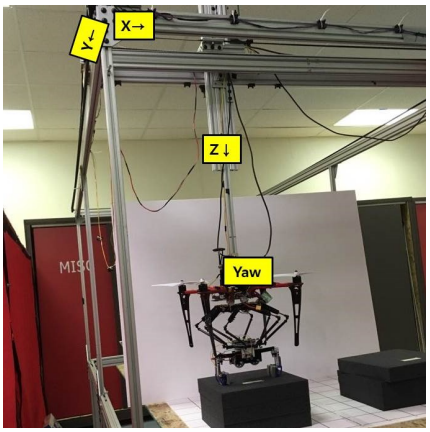

(a) SISTR Gantry System

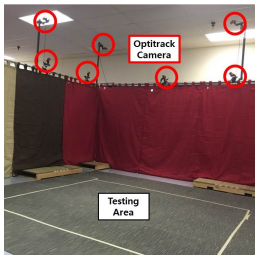

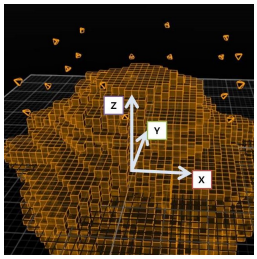

(b) Optitrack Motion Capture System (c) Motion capture volume

Fig. 6. Two test environments

within the limited workspace under the quadcopter ($25cm$ high). To enable this, the relationship between D_1 and D_2 was calculated in Eq. 4

$$D_1 = ||k_i^* - b_i||, \tag{4}$$

where:

$$k_i^* = \begin{bmatrix} k_{xi}^* \\ k_{yi}^* \\ k_{zi}^* \end{bmatrix} = \begin{bmatrix} D_1 \cos(\psi_{bi} \pm \gamma_i)\cos(\theta_i) + b_{xi} \\ D_1 \sin(\psi_{bi} \pm \gamma_i)\cos(\theta_i) + b_{yi} \\ D_1 \sin(\theta_i) + b_{zi} \end{bmatrix} \tag{5}$$

with $\theta_i = 0$.

C. Test Environments

Two test environments are built for lab automation drone concept design testing. The first is a gantry crane system, and the second is a motion-capture space area.

The 4-DOF gantry in Fig. 6(a) was built following Systems Integrated Sensor Test Rig(SISTR) from [13]. The gantry's

$$1.2m \times 0.5m \times 0.5m$$

workspace has the footprint to emulate a small HTS or a larger section of HTS. The gantry runs Dynamixel motors to provide end-effector cartesianal (x,y,z) position and yaw ψ orientation. The concept lab automation drone is affixed to the gantry's end-effector for micro-plate grasping.

The Optitrack motion-capture system is built as in Fig. 6(b), 6(c). The system has $6m \times 6m \times 2.4m$ space. 17 Optitrack Flex3 cameras are connected to a PC running Optitrack Motive Body Software. The calculated motion

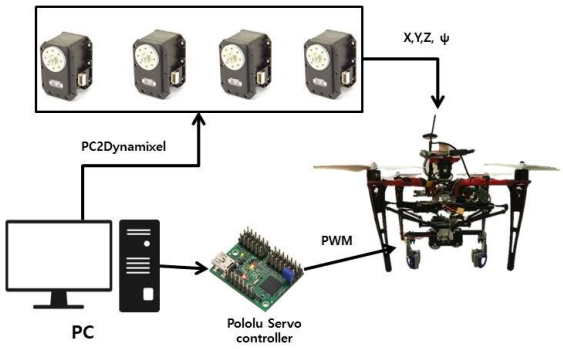

Fig. 7. Gantry Affixed LAD control scheme

capture volume is $3m \times 3m \times 1.8m$. The position data is recorded in real-time by the software.

IV. Test and Evaluation

TABLE V
Rotation Angle of Revolute Joint

Positions			
Pick-up		Store and Delivery	
Joint(i)	$\theta_i(radians)$	Joint(i)	$\theta_i(radians)$
1-8	0.6881	1-8	0.0015

For the testing and evaluation, the lab automation drone concept (LAD) is deployed in two environments for micro-plate pick-and-place. The parallel manipulator-and-gripper (PMG) is set to descend $10cm$ for micro-plate pick-and-place. Table V describes revolute joint angles on each leg during the test.

While the LAD is affixed to the gantry system, there is no motor spinning. A $90cm \times 80cm$ rectangular coordinate system is placed below the LAD to measure translation accuracy. Fig. 7 shows control scheme. First, The parallel manipulator-and-gripper(PMG) descends for micro-plate pick up. Second, the gantry is controlled to drive LAD to the destination by Dynamixels. Then, the PMG place the micro-plate on the destination. During the test, the micro-plate is delivered from (80,20,15) cm to (20,20,15) cm in the gantry system. The result of micro-plate delivery is shown in Fig. 8.

In the motion capture system, the LAD is deployed to fly manually. Fig. 9 shows control scheme. Each Optitrack Tracker is attached on the center of drone frame, and center of micro-plate (Fig. 10). There are four Optitrack Trackers placed on the floor to prescribe a destination in $30cm \times 30cm$ square. First, the LAD is parked on two boxes. Second, the PMG descends to lift the micro-plate. Third, LAD is powered to manually fly to the destination. During the flight, Optitrack Cameras capture the tracker motions, then transmit the data to PC. Fig. 11 shows the trajectories from LAD manual test flight. Green-colored trajectory describes

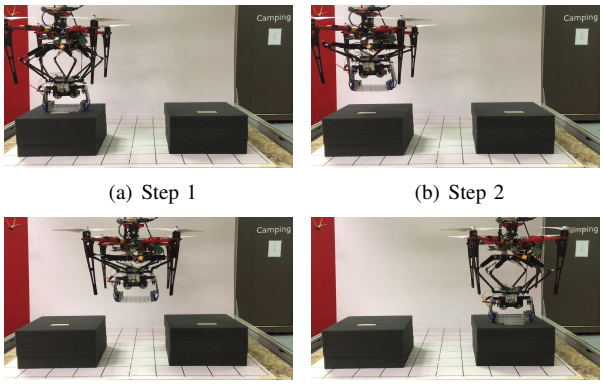

(a) Step 1 (b) Step 2

(c) Step 3 (d) Step 4

Fig. 8. Gantry affixed LAD micro-plate delivery

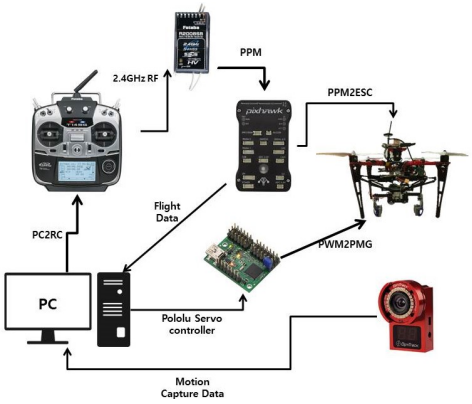

Fig. 9. LAD manual control scheme

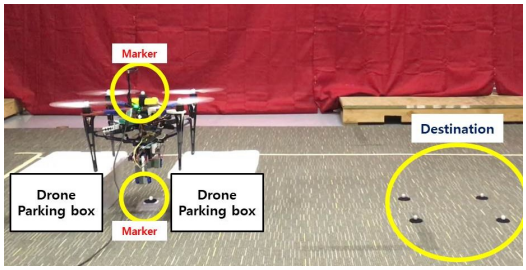

Fig. 10. Gantry affixed LAD control scheme

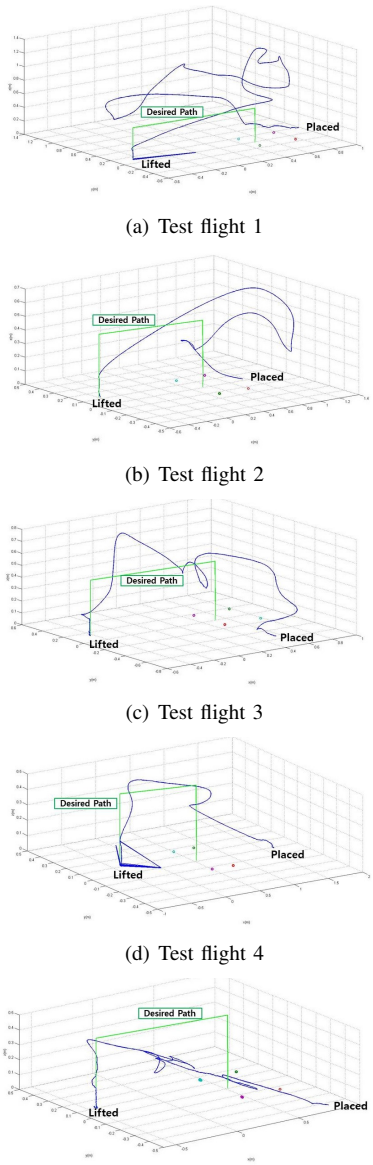

(a) Test flight 1

(b) Test flight 2

(c) Test flight 3

(d) Test flight 4

(e) Test flight 4

Fig. 11. Micro-plate trajectories from LAD manual test flight

desired path. In the previous work [4], the manipulator-gripper itself shows 95 percent precisio in pick-and-place when operated from a gantry. However, the performance was much worse when the entire UAS was deployed. The micro-plate are hard to place on the destination square because of the LAD's flight instability. These results suggest focusing on research areas such as drone dynamic stabilization with parallel manipulator, torque feedback on UAV's positioning from parallel manipulator, and autonomous path planning in future work.

V. Conclusions

In this paper, lab automation drone design concept(LAD) with 6 degree-of-freedom parallel manipulator and sensorized gripper is deployed in two testing environments. First, the LAD is affixed to the gantry system for pick-and-place trials with micro-plates. Second, the LAD is deployed for manual test flight to deliver micro-plates to a desired point in the motion capture area. The results leave much to be desiredin the way of performance, and more work is required in the areas of drone dynamic stabilization with parallel manipulator, torque feedback on UAV's positioning from parallel manipulator, and autonomous path planning.

With improved lab automation drone stabilization and indoor autonomous flight, soon UAS will be ready for missions from National Institutes of Health(NIH) [3]. Next steps will include development of:

- Self-contained motor/drive system
- Built in stabilization/control system
- Wireless communication system
- Sensing capabilities to perform onboard in-room navi-

gation

- Lift and payload capability to support a gripper assembly and the weight of a microplate with a lid
- Expansion capability to add additional on-drone computing capabilities as required to enable in-room navigation and control of the gripper assembly

REFERENCES

[1] Sneader, Walter (1985) Drug Discovery: The Evolution of Modern Medicines. John Wiley and Sons, New York, NY

[2] William P. Janzen (2002) High Throughput Screening : Methods and Protocols. Humana Press

[3] National Institutes of Health/National Center For Advancing Translational Sciences(NIH/NCATS) 015, "Development of a Drone to be used in Laboratory Automation Projects.", U.S. Department of Health and Human Services (HHS), The National Institutes of Health (NIH) and The Centers for Disease Control and Prevention (CDC) Small Business Innovation Research (SBIR) Program, Program Solicitation PHS 2017-1

[4] D. Kim, P. Y. Oh, "Lab Automation Drones for Mobile Manipulation in High Throughput Systems", in Consumer Electronics(ICCE), 2018 International Conference on., IEEE, 2018

[5] S. Michael, D. Auld, C. Klumpp, et al., "Technology Review - A Robotic Platform for Quantative High-Throughput Screening.", ASSAY and Drug Development Technologies, Volume 6, Number 5, 2008, DOI: 10.1089/adt.2008.150
Available : http://lifesciences.tecan.com/products/

[6] RX160 6-axis industrial robot, STAUBLI[Online]
Available : https://www.staubli.com/en/robotics/6-axis-scara-industrial-robot/medium-payload-6-axis-robot/6-axis-industrial-robot-rx160/

[7] M. Orsag, C. Korpela, S. Bogdan, and P. Y. Oh, "Valve turning using a dual-arm aerial manipulator," in Unmanned Aircraft Systems(ICUAS), 2014 International Conference on. IEEE, 2014, Pp. 836-841

[8] T. W. Danko and P.Y. Oh, "Design and control of a hyper-redundant manipulator for mobile manipulating unmanned aerial vehicles," Journal of Intelligent and Robotics Systems, 2013, pp. 1-15

[9] D. Mellinger, Q. Lindsey, M. Shomin, and V. Kumar, "Design, modeling, estimation and control for aerial grasping and manipulation," in Intelligent Robots and Systems(IROS), 2011 IEEE/RSJ International Conference on. IEEE, 2011, pp. 2668-2673

[10] V. Ghadiok, J. Goldin, and W. Ren, "Autonomous Indoor Aerial Gripping Using a Quadrotor," in Intelligent Robots and Systems(IROS), 2011 IEEE/RSJ International Conference on. IEEE, 2011, pp. 4645-4651

[11] Q. Lindsey, D.Mellinger, and V. Kumar, "Construction of cubic structures with quadrotor teams," Proc. Robotics: Science and Systems VII, 2011

[12] J. Sedden, Ph.D. (1990), Basic Helicopter Aerodynamics

[13] C. Korpela, T. W. Danko, and P. Y. Oh, "Designing a System for Mobile Manipulation from an Unmanned Aerial Vehicle," Technologies for Practical Robot Applications (TePRA), 2011 IEEE Conference on. IEEE, 2011, pp. 109-114

[14] T. W. Danko, K. P. Chaney, and P. Y. Oh, "A Parellel Manipulator for Mobile Manipulating UAVs," Technologies for Practical Robot Applications (TePRA), 2015 IEEE International Conference on. IEEE 2015, pp.1-6

[15] F. Szufnarowski, "Stewart platform with fixed rotary actuators a low cost design study," Advances in Medical Robotics, 2013